

RETROSPECTIVE CORRECTIONS FOR 3D FMRI: RETROICOR OR RETROKCOR?

Rob H.N. Tijssen^{1,2}, and Karla L. Miller¹

¹FMRI Centre, Oxford University, Oxford, United Kingdom, ²University Medical Center Utrecht, Utrecht, Netherlands

Introduction Physiological noise, if unaccounted for, can drastically reduce statistical significance of detected activation in FMRI in regions like the brainstem. One common approach is to use externally recorded cardiac and respiratory waveforms to create “nuisance regressors”. The corrections can either be performed in k-space (often referred to as RETROKCOR [1]) or in image space (RETROICOR [2]). Because image space corrections can be incorporated directly into FMRI analysis and the RETROKCOR method was reported to introduce spatial correlations in its correction [2], RETROICOR is often the method of choice for 2D FMRI data. However, RETROICOR requires an appropriate cardiac and respiratory phase for each acquired image. For 3D multi-shot acquisitions, in which the image is reconstructed from data acquired over several seconds, this phase is less well defined. For these sequences it might be more appropriate to perform the correction in k-space, such that each ‘shot’ can be assigned a unique cardiac and respiratory phase. Previous work proposed RETROICOR in 3D FMRI acquisitions by designating the time at which the centre of k-space is collected as the cardiac/respiratory phase for the entire volume [3]. To our knowledge, however, no comparison of image- and k-space corrections for 3D FMRI has been reported. The aim of this work is to optimize and compare retrospective corrections on 3D brainstem FMRI. Simulations are used to characterize and optimize RETROICOR and RETROKCOR and both methods are compared *in vivo* by testing a range of regressors typically used in retrospective corrections.

Methods *Simulations:* Assuming infinite signal-to-noise ratio (SNR) the two corrections are identical if each time point (i.e. k-space or image) is instantaneously sampled, such that a single physiological phase can be assigned to the entire volume. Simulations were therefore performed in which a single-slice acquisition was simulated that critically sampled the respiratory waveform. 329 time-points were generated using a digital 2D Shepp-Logan phantom to which different levels of complex noise was added (SNR=10, 25, 50, and 100). Signal fluctuations mimicking respiratory noise were added in predefined locations (i.e., the mask in Fig. 1(a)). The magnitude was set to obtain a range of contrast-to-noise ratios (CNR = 1, 2.5, 5, and 10). Regressions using the original respiratory waveform as the regressor were performed on the image data (RETROICOR) and k-space data (RETROKCOR).

In vivo comparison: 3D balanced SSFP (bSSFP), and spoiled gradient echo (SPGR) data were acquired in four healthy volunteers on a 3T Siemens TIM TRIO system using a 12-channel head coil. SPGR and bSSFP data were acquired with the following parameters: $\alpha=30^\circ$, TR/TE=12/6, FOV=192x192x48 mm, Matrix=96x96x24, BW=1860 Hz/pix, 8 lines per TR, Tvol = 3.5 s, 60 volumes using a 3D stack-of-segmented EPI readout [4]. Additionally, multi-slice GRE-EPI data were acquired: $\alpha=90^\circ$, TR=3500, TE=30 ms, FOV=192x192x48 mm, Matrix=96x96x24, BW=1860 Hz/pix, 8 lines per TR, 60 volumes. The cardiac and respiratory waveforms were recorded using a plethysmograph and pneumatic bellows to create a set of 18 regressors based on the cardiac and respiratory phase; three orders of Fourier series for the cardiac terms, four orders for the respiratory terms, and first-order interactions [5]. Additionally cardiac and respiratory rate regressors [6,7] were included along with their temporal derivative to allow for temporal shifts. Table 1 lists all the regressors tested. The data were assessed on the temporal stability in a region of interest covering in the brainstem. Table 1 lists all the regressors tested. The data were assessed on the temporal stability in a region of interest covering in the brainstem.

Results and Discussion Figure 1 shows the difference in simulated tSNR after correction with various modifications of the RETROKCOR method (b–e). When RETROKCOR is performed on the phase and magnitude data, as initially proposed by Hu *et al.*, reductions in tSNR are observed at random locations throughout the image (b). This is caused by the high uncertainty of the phase data at k-space locations with low signal magnitude (the edges of k-space). The regressions at these locations are therefore not robust, which can lead to amplification of the noise. Masking the k-space data to exclude k-space locations that have low signal ((c) and (d)) reduces this effect, but also reduces the spatial resolution of the correction [2]. As a result voxels directly adjacent to regions with simulated physiological noise shows reduced tSNR (i.e. the blue rings around the red regions). When the corrections are performed on the real and imaginary channels, however, the correction is improved without the need to mask k-space (Panel (e)). Figure 2 shows *in vivo* results on multi-slice GRE-EPI and 3D bSSFP and SPGR data. The fractional residual variance in the brainstem is shown after individual regressions with each of the regressors listed in Table 1. For each sequence, the largest reduction in variance is obtained by the cardiac regressors (#1–#6). 3D multi-shot readouts, however, are more prone to cardiac fluctuations than single-shot EPI [8], hence the larger effect of the cardiac regressors in 3D bSSFP and SPGR compared to 2D GRE-EPI. It is interesting that RETROICOR appears to perform equally well as, and for some regressors even better than, RETROKCOR in 3D bSSFP and 3D SPGR, indicating that a single regressor for the entire volume is sufficient to model physiological fluctuations. Further, many regressors have little effect, and their inclusion may actually be detrimental due to reduced degrees-of-freedom (discussed in a separate abstract).

Conclusions In this work we have shown that RETROKCOR corrections are considerably improved when the corrections are performed on the real and imaginary channels instead of the phase and magnitude. When comparing the performance of RETROICOR and RETROKCOR on 3D resting data, it is observed that RETROICOR performs equally well as RETROKCOR. This has considerable practical implications as the use of RETROICOR removes the need for off line reconstruction of k-space data.

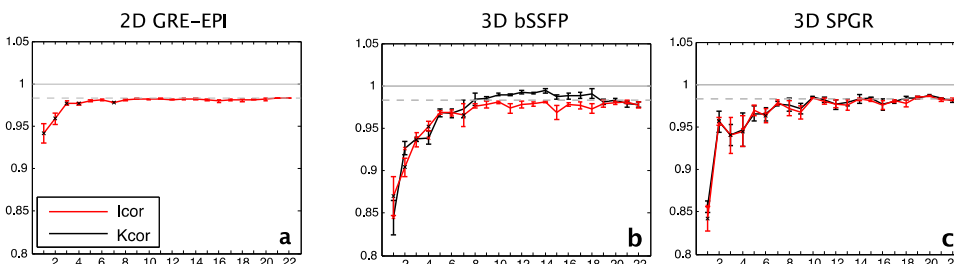


Figure 2: The residual variance after regression with each of the regressors individually. The variance is normalized against the variance in the data without retrospective correction. The dashed line represents the expected residual variance when the regression is performed using a randomly constructed regressor.

References [1] Glover, MRM, 2000. [2] Hu, MRI, 1995. [3] Lutti, Proc. ISMRM, 2011 [4] Miller, MRM, 2006. [5] Brooks, NIMG, 2008. [6] Birn, NIMG, 2006 [7] Shmueli, NIMG, 2007 [8] Tijssen, NIMG 2011.

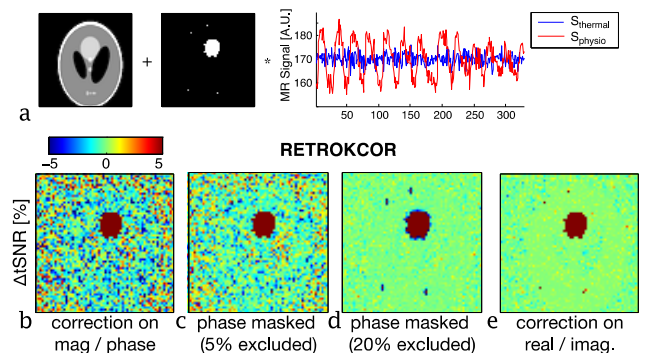


Figure 1: RETROKCOR results on simulated 2D data (SNR=25, CNR=2.5). a) Simulation pipeline, b–e) tSNR difference in magnitude image data.

Table 1: Description of the set of regressors.

No.	Name	Description
1	ev01.cards0.01	cardiac: First order cosine
2	ev02.cardsin.01	cardiac: First order sine
3	ev03.cards0.02	cardiac: Second order cosine
4	ev04.cardsin.02	cardiac: Second order sine
5	ev05.cards0.03	cardiac: Third order cosine
6	ev06.cardsin.03	cardiac: Third order sine
7	ev07.resp0.01	Respiratory: First order cosine
8	ev08.resp0.01	Respiratory: First order sine
9	ev09.resp0.02	Respiratory: Second order cosine
10	ev10.resp0.02	Respiratory: Second order sine
11	ev11.resp0.03	Respiratory: Third order cosine
12	ev12.resp0.03	Respiratory: Third order sine
13	ev13.resp0.04	Respiratory: Fourth order cosine
14	ev14.resp0.04	Respiratory: Fourth order sine
15	ev15.cosadd	Interaction: (card + resp) cosine
16	ev16.cossub	Interaction: (card – resp) cosine
17	ev17.sinadd	Interaction: (card + resp) sine
18	ev18.sinsub	Interaction: (card – resp) sine
19	ev19.cr	Cardiac rate
20	ev20.dcr	Cardiac rate derivative
21	ev21.rvt	Respiratory rate
22	ev22.drvt	Respiratory rate derivative